International Soil and Water Conservation Research 4 (2016) 293–303

HOSTED BY

Contents lists available at ScienceDirect

International Soil and Water Conservation Research

journal homepage: www.elsevier.com/locate/iswcr

Original Research Article

Spatial distribution of heavy metals in the middle nile delta of Egypt☆

Mohamed S. Shokr[a,b,*], Ahmed A. El Baroudy[a], Michael A. Fullen[b], Talaat R. El-beshbeshy[a], Ali R. Ramadan[c], A. Abd El Halim[a], Antonio J.T. Guerra[d], Maria C.O. Jorge[d]

[a] Soils and Water Department, Faculty of Agriculture, Tanta University, Tanta, Egypt
[b] The University of Wolverhampton, Wolverhampton WV1 1LY, UK
[c] Soils and Water Use Department, National Research Centre, Giza, Egypt
[d] Department of Geography, Federal University of Rio de Janeiro, Brazil

ARTICLE INFO

Keywords:
El-Gharbia Governorate
Egypt
Soil contamination
X-ray fluorescence spectrometry
Remote sensing
Geographical information systems
Indices calculations

ABSTRACT

Heavy metal contamination in the El-Gharbia Governorate (District) of Egypt was identified by using remote sensing, Geographical Information Systems (GIS), and X-ray fluorescence (XRF) spectrometry as the main research tools. Digital Elevation Model (DEM), Landsat 8 and contour map images were used to map the landforms. Different physiographic units in the study area are represented by nine soil profiles. X-ray fluorescence spectrometry (XRF) was used for geochemical analysis of 33 soil samples. Vanadium (V), nickel (Ni), chromium (Cr), copper (Cu) and zinc (Zn) concentrations were measured and they all exceeded the average global concentrations identified by Wedepohl (1995). Ni and Cr concentrations exceeded recommended values in all soil profile horizons (Canadian Soil Quality Guidelines, 2007), while Cu had a variable distribution. Zn concentrations are under recommended concentration limits in most soil samples. Contamination Factor, Pollution Load Index and Degree of Contamination indices were used to assess the environmental risks of heavy metal contamination from the soils. All analysed metals pose some potential hazard and pollution levels were particularly high near industrial and urban areas.

1. Introduction

Heavy metals are considered as one of the most critical contaminants in the environment, because of their toxicity, persistence and bio-accumulation. These elements can bio-accumulate in plants, animals and humans via the food chain (Abrahams, 2002). The Nile Delta is one of the oldest intensely cultivated areas on earth and is very densely populated, with ≤1,600 inhabitants per square kilometre (Zeydan, 2005). Agricultural development, industrial activities and inadequate rural sanitation have considerable impacts on eutrophication and contamination status, ecological value and environmental conditions on the Nile Delta (Zeydan, 2005).

Natural and anthropogenic activities are two important sources of heavy metals in soil. Natural sources of heavy metals include weathering and other pedogenic processes acting on rock fragments, and are usually at relatively low concentrations (Baltrėnas, Jankaitė, & Kazlauskienė, 2008; Anikwe & Mbah 2010). Commercial fertilizers, liming materials, agrochemicals and other materials used as soil amendments, irrigation water and atmospheric decomposition are the main anthropogenic sources of heavy metals in soils (Baldassarre, Radina, Senesi, & Senesi, 1999; Filippidis, Michailidis, Mladenova, & Sofianska, 2013). The continuous application of mineral fertilizers which contain high heavy metal concentrations pose potential health threats (Abdelhafez et al., 2012).

Heavy metals become soil contaminants for several reasons. Firstly, their rates of generation by human activities are more rapid than natural ones. Secondly, the chemical form of metal in the receiving environmental system usually make it more bioavailable. Thirdly, where higher potential of direct exposure occurs they can be transferred from sources (usually mines) to diffuse environmental locations (Al-Abed, D'Amore, Ryan, Scheckel & 2005). Heavy metals are usually adsorbed by soil, firstly by initial rapid reactions for minutes or hours, followed by slow adsorption reactions for days or years. Thus, heavy metals can be redistributed into different chemical forms, with associated variations in bioavailability, mobility and toxicity (Buekers, 2007). Heavy metals in soil due to human activities are usually more mobile compared with pedogenic or lithogenic forms (Kaasalainen & Yli-Halla, 2003).

The use of Geographical Information Systems (GIS) is one of the most efficient tools for studying environmental geochemistry (Jiao, Lu,

Peer review under responsibility of International Research and Training Centre on Erosion and Sedimentation and China Water and Power Press.
* Corresponding author.
E-mail address: m.s012@yahoo.com (M.S. Shokr).

http://dx.doi.org/10.1016/j.iswcr.2016.10.003
Received 4 September 2016; Received in revised form 30 October 2016; Accepted 31 October 2016
Available online 15 November 2016

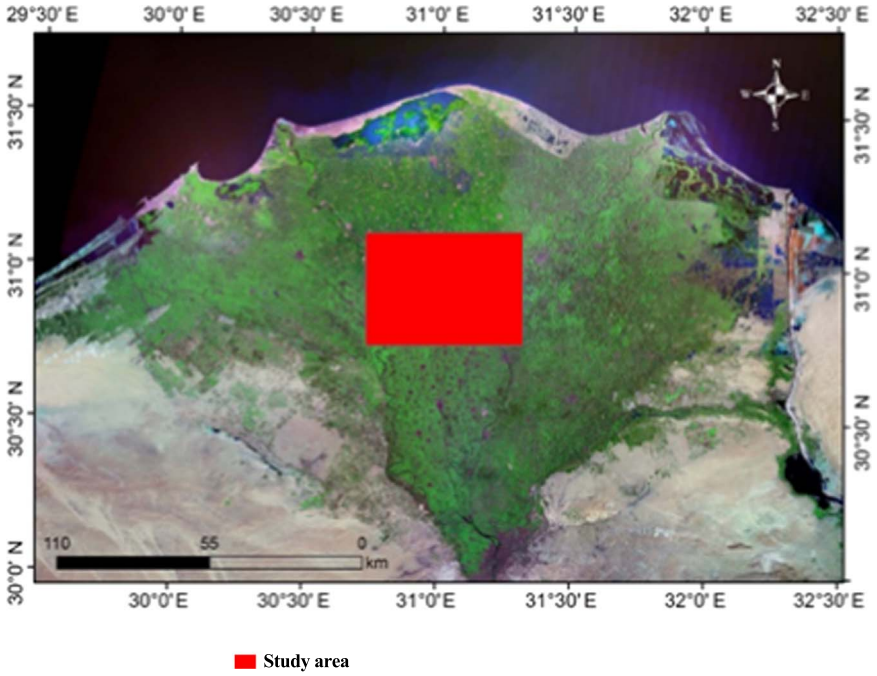

Fig. 1. Location of the study area in the middle Nile Delta of Egypt.

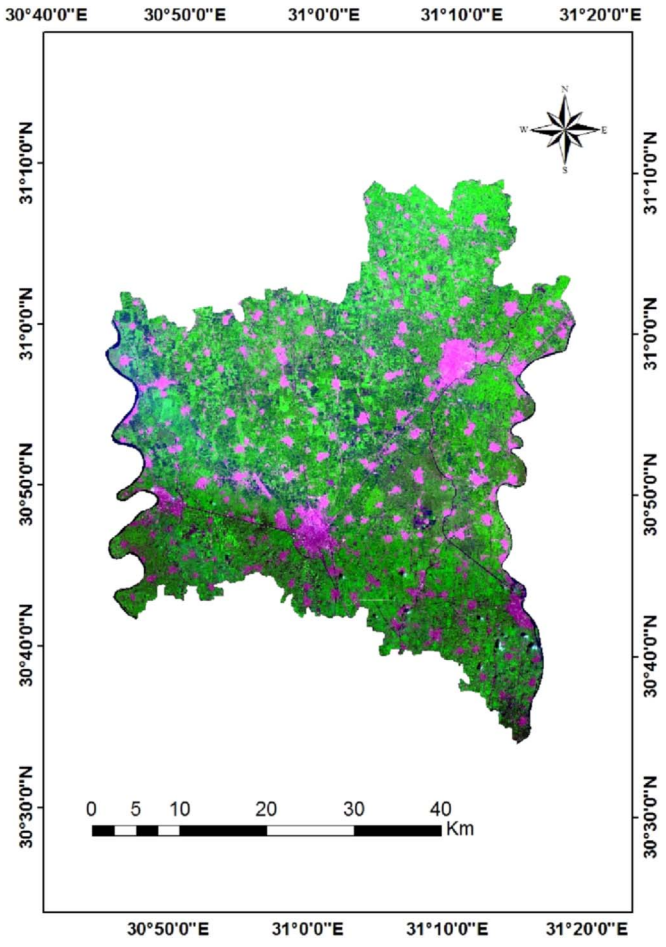

Fig. 2. Landsat 8 mosaic of the study area.

Teng, Wu & Wang, 2014). Spatial distribution is essential for assessment of effects of heavy metals on soil and to delineate contamination zones (El Razek & Omran, 2012). The use of inverse distance weight (IDW) procedures can assist spatial interpolation of heavy metal distribution patterns (Zheng, 2006).

The spatial interpolation of IDW can produce maps of heavy metal distributions and quantify the probability of heavy metal concentrations higher than their guide values (Bhalli, Ghaffar, Parveen & Shirazi, 2012). The identification of appropriate reference values for uncontaminated soil conditions is a major methodological problem associated with correctly assessing soil contamination, as all quantitative assessment methods rely on reference values exceeding background concentrations (Desaules, 2012). The most common reference values used for soil contamination assessment are background, crustal and regulatory reference values.

Both quantitative and qualitative methods are used for soil contamination assessment. Qualitative methods are inferential and indicative and multivariate analyses require that each variable is normally distributed and that the whole data-set has a multivariate normal distribution (de Caritat & Reimann, 2000). The Contamination Factor (CF) is one of the most commonly used quantitative methods used to evaluate the severity of heavy metal contamination. CF has been applied to assess the roles of anthropogenic sources in contaminating sediments with heavy metals in the Jinix River Catchment of China (Abdelhafez & Li, 2014).

The main aim of the present study is to identify the distribution of selected heavy metals in El-Gharbia Governorate, using remote sensing, Geographical Information Systems (GIS) and X-ray fluorescence (XRF) spectrometry.

2. Materials and methods

2.1. Study area

The study area is the Middle part of the Nile Delta of Egypt (30°45′20″–31°10′50″E;30°35′10″–31°10′05″N) and covers an area

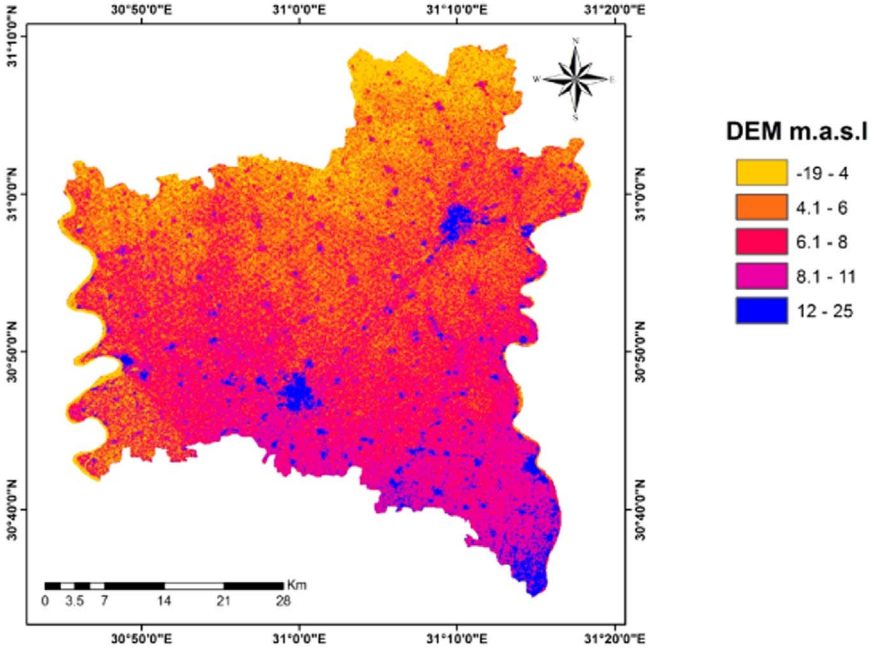

Fig. 3. Surface elevation of study area as extracted from the SRTM data and contour maps.

Table 1
The Contamination factor (CF) for assessing contamination levels in soil.
Source: Hakanson (1980).

Contamination Factor (CF)	Classification
CF < 1	Low contamination
1≤CF < 3	Moderate contamination
3≤CF < 6	Considerable contamination
CF≥6	Very high contamination

Table 2
Degree of contamination and classification.
Source: Caeiro, Costa, and Ramos (2005).

Degree of contamination (DC)	Classification
DC < n	Low contamination
n≤Dc < 2n	Moderate contamination
2n≤Dc < 4n	Considerable contamination
CF≥4n	Highly contaminated

Table 3
Description of the degree of contamination in the Nile Delta study area.

Degree of contamination (Dc)	Classification
DC < 5	Low contamination
5≤Dc < 10	Moderate contamination
10≤Dc < 20	Considerable contamination
DC≥20	Highly contaminated

of 1927.4 km^2 (Figs. 1, 2). Based on the US Soil Taxonomy (USDA, 2010) the local soil temperature regime is Thermic and the soil moisture regime is Torric. The mean monthly temperature reaches its maximum in June, July and August and often exceeds 30 °C. The mean minimum temperature (11.2 °C) usually occurs in January, February or March at Tanta Meteorological Station (Climatologically Normal for Egypt, 2011). Precipitation is unequally distributed through the rainy season. Annual rainfall is very low and mostly falls in winter; with a mean 3.8 mm/year. Rain mainly falls in the cold season (November-March) and the minimum amount is in June and September. The area belongs to the late Pleistocene era, which is evidenced by the deposits of the Neonile, which are mainly composed of medium and fine silt (Said, 1993).

2.2. Digital image processing and physiographic mapping

Digital image processing was completed for two Landsat 8 satellite images acquired in May 2014 (path 177/row 38 and path 177/row 39), with a spatial resolution of 30 m. The images were pre-processed, including radiometric correction (used to modify digital values of pixels to remove 'noise'). Images were geometrically rectified using the Universal Transverse Mercator (UTM) co-ordinates, with the World Geodetic System datum (WGS 1984) and then maps were constructed. Images were atmospherically corrected using the FLAASH module (ITT, 2009). Data were calibrated to radiance using the inputs of image type, acquisition date and time. Images were subject to linear stretching by 2%, smooth-filtered, and their histograms were matched, adopting the procedures of Lillesand and Kiefer (2007) and mosaicked using ENVI 5.1 software. The extraction of landform units used high spatial resolution images, so the spatial resolution of satellite image was enhanced using the data merge function of Envi 5.1 software. Merging was performed by using multispectral bands (~30 m) as low spatial resolution, and band 8 (panchromatic band) with ~15 m resolution. Landform topography data were extracted using contour maps (scale 1:25,000) and enhanced satellite images. Both enhanced satellite images were processed using the DEM (Fig. 3) in ERDAS Imagine 8.7, to extract the landform information (Dobos et al., 2002). The initial landform maps were ground-truthed using field observations.

2.3. Spatial distribution of heavy metals

Spatial interpolation is widely used when data are collected at distinct locations (e.g. soil profiles) for producing continuous information (Ali & Moghanm, 2013). Inverse distance weighted (IDW) is an interpolation method, which uses measured values surrounding the prediction location. The measured values closest to the prediction location have more influence on the predicted value than those further away, thus giving greater weight to points closest to the prediction

Table 4
Physiographic units on the soil map.

Physiographic unit	Landform	Mapping unit	Soil profile	Profile elevation (masl)[a]	Area (km^2)	Area (%)
Flood plain	High terraces	T1	9	12	232.21	12.05
	Moderately high terraces	T2	4	8	431.99	22.41
	Low Terraces	T3	1	0	417.80	21.68
	High Decantation Basin	D1	3	10	39.53	2.05
	Low Decantation Basin	D2	5	6	236.29	12.26
	High overflow Basin	OB1	6	7	244.46	12.68
	Low Overflow basin	OB2	7	5	206.45	10.71
	Levees	L	8	9	103.82	5.39
	Swales	S	2	8	14.89	0.77
	Total	–	–	–	1927.44	100.00

1. River terraces: these soils represent the late Pleistocene deltaic plain and occur at the edge of decantation basins (these are basins in which sedimentation, particularly of silt and clay, occurs during floods). The soils are formed on terraces at various heights above the valley floor.
2. Basins: these are artificially enclosed areas of a river or harbour, designed so that water levels are unaffected by tides.
3. River levees: these are a type of dam that runs along the banks of rivers or canals. Levees reinforce the banks and help prevent flooding. By confining the flow, levees can also increase water velocity.
4. Swales: these are low tracts of land, usually consisting of moist and marshy lands. The term can refer to both natural and artificial landscape features. Artificial swales are often designed to manage water runoff, filter pollutants and increase rainwater infiltration.

[a] masl = metres above sea level.

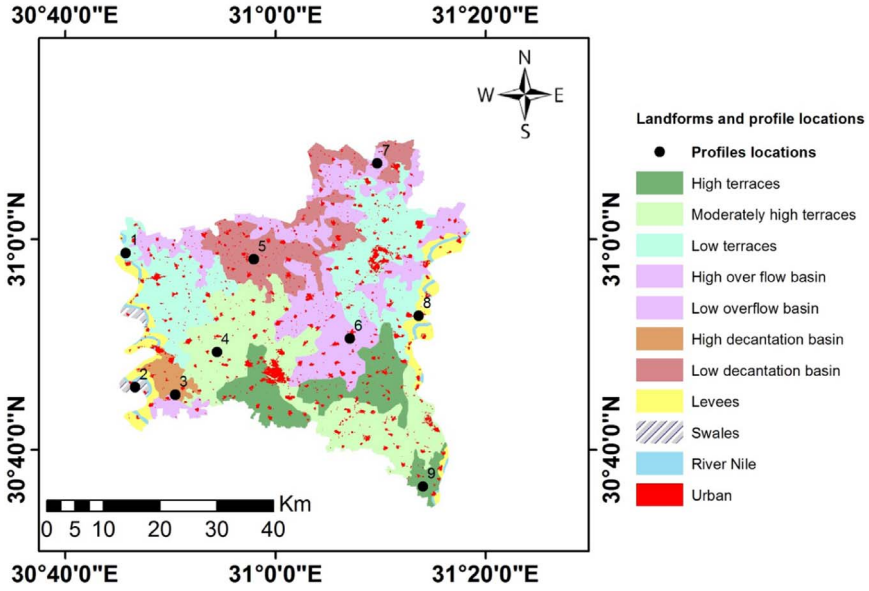

Fig. 4. The main landforms of the study area and profile locations.

location, and the weights decrease as a function of distance (Shepard, 1968). Geostatistical relationships among the known points used ArcGIS 10.1 software to interpolate heavy metal concentrations in the study area. The spatial interpolation method (IDW) was used, with 12 neighbouring samples for estimation of each grid point. A power of two was used to weight the nearest points.

2.4. Soil analysis

Soil samples were collected from nine profiles in El-Gharbia Governorate, representing the different soil units. Pedological descriptions of profiles were conducted using the procedures of FAO (2006). About 1 kg was collected from each horizon of each profile. Three replicate samples were mixed together to make one representative sample. Soil samples were air-dried and large stones and organic debris were removed before sieving. Samples were gently ground, homogenized, sieved through a 2.0 mm sieve and then crushed to a fine (< 125 μm) powder. Oven-dry samples were ignited at 375 °C for 16 h (overnight), adopting the procedures of Ball (1964). Subsamples of 8.5 g of soil powder were added to 1.5 g of wax (Lico waxc micropowder PM, Hoechst wax) and then compressed under 12 t pressure using a semi-automatic hydraulic press to make a pellet. The geochemical composition of soil pellets were analysed using an XRF spectrometer model Epsilon3 XLE. XRF analyses were performed at the University of Wolverhampton, UK.

2.5. Assessment of contamination risk

Average values for the upper lithosphere were used as background values to calculate all indices (Wedepohl, 1995).

2.5.1. Contamination factor (CF)

The Contamination Factor (CF) is used to assess contamination by comparing heavy metal concentrations in soils with background values. The calculation of CF uses the equation:

$$CF = C/C0 \quad (1)$$

Where C= the measured concentration of the element in soil.

C0= the geochemical background concentration of the heavy metal.

The following classes are used to describe CF (Table 1).

Table 5
XRF analysis of soils collected from the study area.

Profile no	Mapping unit	Depth (cm)	Metal concentrations (mg/kg)				
			V	Cr	Ni	Cu	Zn
1	T3	0–50	227.1	179.7	68.30	78.60	94.30
		50–85	265.9	158.1	77.80	60.90	85.40
		85–120	250.4	167.3	73.50	81.40	93.30
		120–150	221.8	163.3	61.60	60.10	80.80
2	S	0–45	744.4	519.0	267.30	288.90	377.60
		45–85	244.9	161.4	63.50	50.90	75.50
		85–110	250.8	192.4	70.20	71.40	86.80
3	D1	0–75	221.0	170.7	63.80	94.50	90.20
		75–100	241.4	179.6	63.00	73.00	86.90
		100–150	238.9	166.6	81.60	76.60	85.00
4	T2	0–60	203.1	159.2	72.30	118.70	308.00
		60–100	258.3	166.3	70.90	0.00	88.70
		100–120	222.8	166.2	65.50	75.20	84.90
		120–150	206.1	179.8	70.70	72.30	91.60
5	D2	0–45	194.0	149.1	74.40	95.20	103.10
		45–65	197.5	159.6	69.20	93.30	98.40
		65–110	225.3	143.0	73.20	95.50	95.00
		110–150	205.0	150.5	72.20	94.60	98.80
6	OB1	0–35	210.1	140.3	60.60	131.80	124.50
		35–65	216.0	152.7	76.70	76.40	109.40
		65–100	220.9	164.3	84.50	97.50	103.20
		100–150	219.5	153.7	85.00	0.00	100.60
7	OB2	0–55	228.2	180.8	76.50	93.50	94.70
		55–110	230.3	170.7	73.30	89.10	84.70
		110–150	196.5	168.7	64.50	74.10	84.30
8	L	0–30	218.7	164.1	68.90	0.00	93.20
		30–60	241.3	151.3	73.90	0.00	97.10
		60–100	247.3	155.4	82.10	0.00	89.50
		100–150	231.9	154.9	75.40	85.80	93.80
9	T1	0–45	250.7	156.8	78.20	0.00	112.10
		45–105	232.8	158.1	80.90	74.30	103.30
		105–130	223.7	168.8	76.40	74.50	89.50
		130–150	231.1	168.4	69.70	74.10	94.00

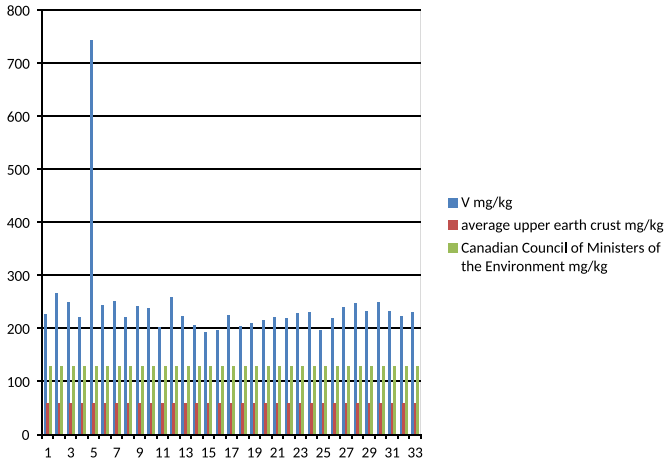

Fig. 5. Vanadium concentrations in soil samples and concentration limits specified by Wedepohl (1995) and CSQG (2007).

2.5.2. Pollution load index (PLI)

The Pollution Load Index (PLI) expresses the quantity of a pollutant in the environment (Harris, Jeffrey, Tomlinson & Wilson, 1980). The PLI of a single site is the nth root of n multiplied by CF, using the equation:

$$PLI = (CF1 \times CF2 \times CF3 \times \cdots\cdots \times CFn)^{1/n} \quad (2)$$

PLI > 1 indicates that the area is polluted and < 1 means the environment is not polluted (Natesan, Deepthi & Seshan, 2010).

2.5.3. Degree of contamination (DC)

DC is the sum of all contamination factors for a given site and is calculated using the equation given by Hakanson (1980):

$$DC = \sum_{1}^{n} CF \quad (3)$$

Where CF= the contamination factor

n= the count of the elements present.

Table 2 summarizes the DC classification.

The following classes were used for the description of the degree of contamination in the study area (Table 3).

Where n = the number of heavy metals (i.e. n=5).

3. Results and discussion

3.1. Physiographic map of the study area

Satellite images show that the study area is a flood-plain and includes high terraces, moderately high terraces, low terraces, high decantation basins, low decantation basins, high overflow basins, low overflow basins, river levees and swales. The main physiographic soil units of the study area are reported in Table 4 and Fig. 4.

3.2. Heavy metal contamination

XRF analyses of soil samples identified the presence of SiO_2, Al_2O_3, P_2O_5, K_2O, CaO, MgO, Na_2O and Fe_2O_3 (major) and Cr, Cu, Zn, Ni, Br, Rb, Sr, Y, Zr, Nb, Sn, Te, Ba, Eu, Yb, Re, Ga, Ir, Mo, As and Pb (minor). Concentrations of the heavy metals Cr, Cu, Ni, V and Zn for each profile are reported in Table 5. For the metals Te, Mo, As and Pb, results are not reported, because their concentrations were below detection limits. Spatial interpolation maps (Figs. 6, 8, 9, 12 and 14) of heavy metal

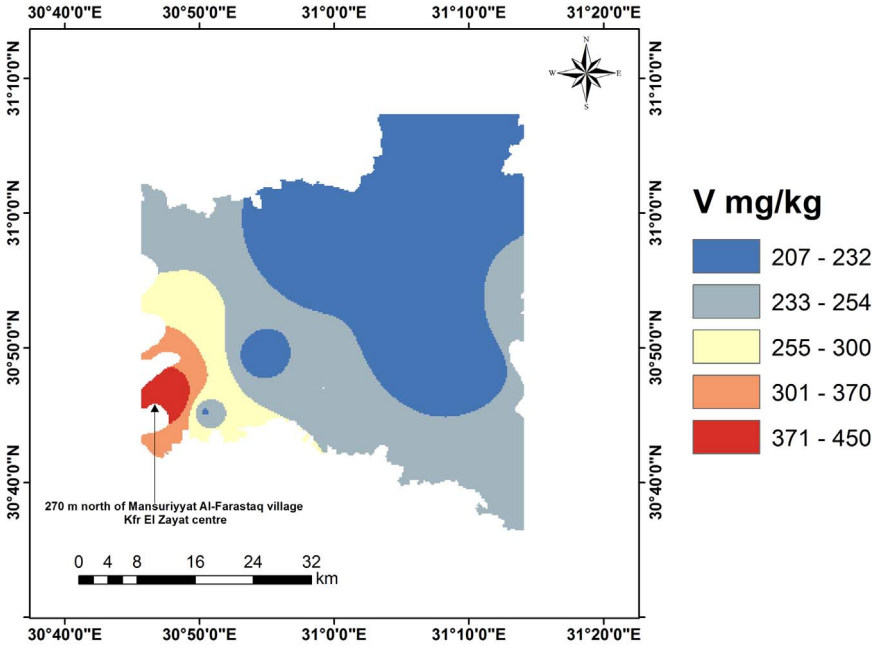

Fig. 6. The interpolated map of weighted mean of vanadium.

Table 6
Heavy metal concentrations of soil samples and concentration limits specified by Wedepohl (1995) and CSQG (2007).

Profile No	Mapping unit	Mean weighted metal concentrations (mg/kg)				
		V	Cr	Ni	Cu	Zn
1	T3	240.53	168.48	70.39	71.42	89.29
2	S	450.58	314.73	148.39	152.92	201.65
3	D1	230.36	170.81	69.60	84.94	87.91
4	T2	221.04	166.14	70.70	71.96	176.49
5	D2	206.79	149.06	72.76	94.87	98.89
6	OB1	216.93	152.84	77.53	68.79	108.54
7	OB2	220.51	173.87	72.12	86.71	88.26
8	L	235.24	156.15	75.58	28.60	93.19
9	T1	236.42	160.86	83.28	52.01	102.40
Average upper earth crust (mg/kg)		60	35	18.60	14.30	52
CSQG (agricultural soil) (mg/kg)		130	64	50	63	200

concentrations were prepared using the IDW function (inverse distance weighted) interpolation method in Arc-GIS 10.1.

3.3. Vanadium

V concentrations are higher than the average values (60 and 130 mg/kg) of the lithosphere (Wedepohl, 1995) and Canadian Soil Quality Guidelines (CSQG), 2007), respectively. The concentrations and the interpolation map for V in the soil samples are given in Table 5 and Figs. 5 and 6. V concentrations ranged from 194.0 to 744.4 mg/kg, with a weighted mean ranging from 206.79 to 450.58 mg/kg (Table 6). The highest measured concentration of V was in the upper horizon of profile 2, which represents a swales unit 270 m north of Mansuriyyat Al-Farastaq village, ~6.5 km south-west from the centre of the town of Kfr Elzayat (population in 2015 was 448,965). CF values range from 3.23 to 12.40 and show that all soil samples are in the 'considerably' and 'very highly contaminated' Classes (Table 7). The high deposition of V might be due to the numerous local factories. The spatial interpolation shows a trend of increasing concentrations from north-east to south-west. The highest weighted mean (weighting concentration by representative area) (450.58 mg/kg) was found in 0.77% of the study area. From the interpolation map of V in the study area (Fig. 6) we can conclude that the ascending order of concentration in the mapping units is: low decantation basin (D2), high overflow basin (OB1), low overflow basin (OB2), moderately high terraces (T2), high decantation basin (D1), levees (L), high terraces (T1), low terraces (T3) and swales (S).

3.4. Chromium

The main natural source of chromium is the flux of continental dust in the atmosphere, but much larger amounts are released by human activities (El-Bady, 2014). The highest concentration of Cr (519 mg/kg) was in the top-soil of Profile 2, which may be contaminated from local factories. The lowest concentration (140.3 mg/kg) was in the top-soil of Profile 6, which represents a high over-flow basin (Table 5), where the mean weighted Cr concentrations ranged from 152.84 to 314.73 mg/kg (Table 6). All concentrations markedly exceeded the values given by both Wedepohl (1995) and CSQG (2007) (Fig. 7). According to CF values, all soil samples are in the 'considerably' and 'very highly' contaminated Classes (Table 7). Cr concentrations increased from east to west and south of the study area (Fig. 8). The highest Cr concentrations tended to be in the swales unit and the lowest in the high overflow basin unit.

Table 7
Contamination Factor (CF) and soil contamination levels.

Profile no	Depth (cm)	V	C Level	Cr	C Level	Ni	C Level	Cu	C Level	Zn	C Level
1	0–50	3.79	C	5.13	C	3.67	C	5.50	C	1.81	M
	50–85	4.43	C	4.52	C	4.18	C	4.26	C	1.64	M
	85–120	4.17	C	4.78	C	3.95	C	5.69	C	1.79	M
	120–150	3.70	C	4.67	C	3.31	C	4.20	C	1.55	M
2	0–45	12.41	VH	14.83	VH	14.37	VH	20.20	VH	7.26	VH
	45–85	4.08	C	4.61	C	3.41	C	3.56	C	1.45	M
	85–110	4.18	C	5.50	C	3.77	C	4.99	C	1.67	M
3	0–75	3.68	C	4.88	C	3.43	C	6.61	VH	1.73	M
	75–100	4.02	C	5.13	C	3.39	C	5.10	C	1.67	M
	100–150	3.98	C	4.76	C	4.39	C	5.36	C	1.63	M
4	0–60	3.39	C	4.55	C	3.89	C	8.30	VH	5.92	C
	60–100	4.31	C	4.75	C	3.81	C	0.00	L	1.71	M
	100–120	3.71	C	4.75	C	3.52	C	5.26	C	1.63	M
	120–150	3.44	C	5.14	C	3.80	C	5.06	C	1.76	M
5	0–45	3.23	C	4.26	C	4.00	C	6.66	VH	1.98	M
	45–65	3.29	C	4.56	C	3.72	C	6.52	VH	1.89	M
	65–110	3.76	C	4.09	C	3.94	C	6.68	VH	1.83	M
	110–150	3.42	C	4.30	C	3.88	C	6.62	VH	1.90	M
6	0–35	3.50	C	4.01	C	3.26	C	9.22	VH	2.39	M
	35–65	3.60	C	4.36	C	4.12	C	5.34	C	2.10	M
	65–100	3.68	C	4.69	C	4.54	C	6.82	VH	1.98	M
	100–150	3.66	C	4.39	C	4.57	C	0.00	L	1.93	M
7	0–55	3.80	C	5.17	C	4.11	C	6.54	VH	1.82	M
	55–110	3.84	C	4.88	C	3.94	C	6.23	VH	1.63	M
	110–150	3.28	C	4.82	C	3.47	C	5.18	C	1.62	M
8	0–30	3.65	C	4.69	C	3.70	C	0.00	L	1.79	M
	30–60	4.02	C	4.32	C	3.97	C	0.00	L	1.87	M
	60–100	4.12	C	4.44	C	4.41	C	0.00	L	1.72	M
	100–150	3.87	C	4.43	C	4.05	C	6.00	VH	1.80	M
9	0–45	4.18	C	4.48	C	4.20	C	0.00	L	2.16	M
	45–105	3.88	C	4.52	C	4.35	C	5.20	C	1.99	M
	105–130	3.73	C	4.82	C	4.11	C	5.21	C	1.72	M
	130–150	3.85	C	4.81	C	3.75	C	5.18	C	1.81	M

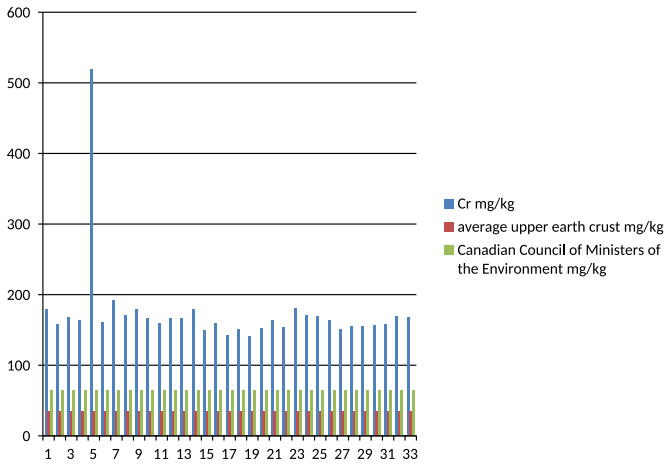

Fig. 7. Chromium concentrations in soil samples and concentration limits specified by Wedepohl (1995) and CSQG (2007).

3.5. Nickel

Ni concentrations ranged from 60.60 to 267.3 mg/kg (Table 5), with weighted mean concentrations ranging from 69.6 to 148.39 mg/kg (Table 6). The spatial trends showed that concentrations increased from north to south and west. The interpolation of Ni shows high spatial variability, with the lowest values in the high decantation basin units and the highest concentrations in swales, which occupy 14.89 km^2 of the study area (Fig. 9). Ni concentrations were higher than the limits (18.60 and 50 mg/kg) specified by Wedepohl (1995) and CSQG (2007), respectively (Fig. 10) and exceeded the concentrations of previous studies in Egyptian alluvial soils (64.4 mg/kg) by Baghdady and Sippola (1984). The CF of all samples are in the 'considerably' and 'very highly' contaminated classes (Table 7).

3.6. Copper

The two main sources of Cu on the Nile Delta are applications of: (1) Cu-based liquid fungicides, and (ii) $CuSO_4$ as an algicide in treating problematic macro-algal blooms in the Nile, especially during summer (Abdel-Moati & El-Sammak, 1997). The weighted mean concentrations ranged from 28.9 to 152.92 mg/kg (Table 6). Most concentrations exceeded the limits of 14.3 and 63 mg/kg specified by Wedepohl (1995) and CSQG (2007), respectively (Fig. 11). However, the concentrations of the second horizon of Profile 4; and the first, second and third horizons of Profile 8 were less than the specified limits. In Profile 9, the deepest horizon exceeded the limit, whereas the concentration in the upper layer was 0 mg/kg (Table 5). This is probably due to percolation and illuviation of Cu, associated with irrigation water. These profiles represent moderately high terraces, levees and high terraces, respectively. The CF values showed that soil samples were in three contamination classes ('low,' 'considerable' and 'very highly contaminated') (Table 7). The lowest Cu concentrations were in the river levee units and the highest values were in the swales units (Fig. 12).

3.7. Zinc

Zn concentrations are higher than the 52 mg/kg average of the upper lithosphere (Wedepohl, 1995) and lower than the maximum permissible value of 200 mg/kg (CSQG, 2007). The exceptions are the upper horizons of Profiles 2 and 4, where their concentrations greatly exceeded permissible limits (377.6 and 308 mg/kg, respectively) (Table 5, Fig. 13). All of the highest concentrations were in the upper horizon, but the highest concentration in Profile 8 was in the sub-soil (Table 5). This could be caused by infiltration of irrigation water

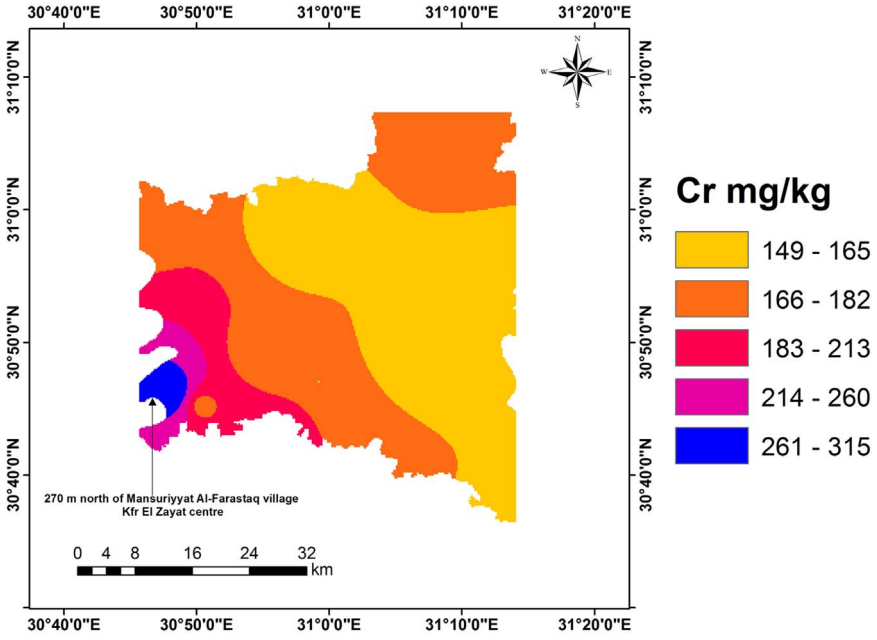

Fig. 8. The interpolated map of weighted mean of chromium.

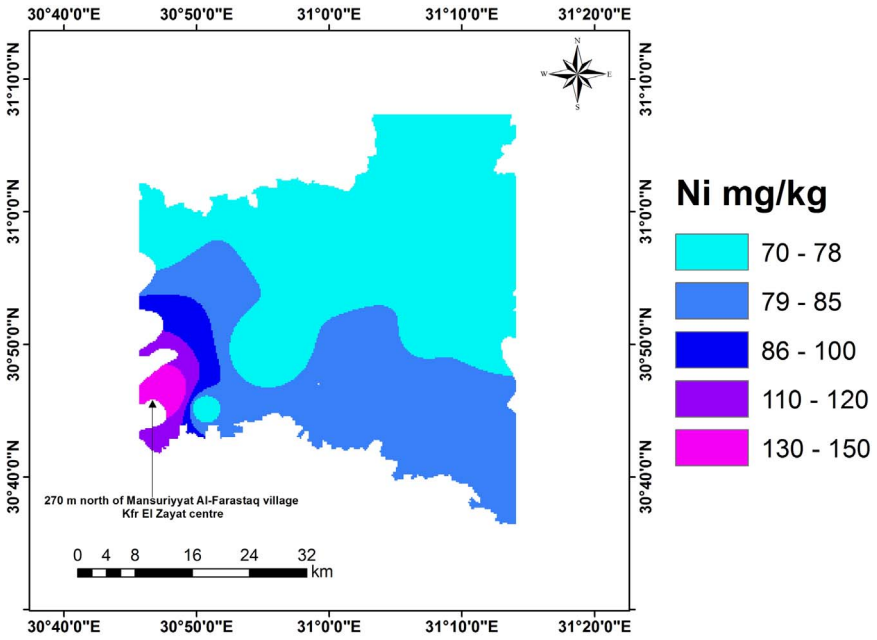

Fig. 9. The interpolated map of weighted mean of nickel.

through the profile. The weighted mean Zn concentration ranged between 88.26–201.65 mg/kg (Table 6). According to the CF values, the Zn concentrations of all soil samples fell into the 'moderately contaminated class,' except for the first horizons of Profiles 2 and 4, which were in the 'very high contaminated' and 'considerably' contaminated classes, respectively (Table 7). The highest concentration was in the south-west of the study area, which is located 270 m north of Mansuriyyat Al-Farastaq village (Fig. 14). This could be due to atmospheric deposition, originating from local industrial plants. The highest Zn concentrations were in swale top-soils and moderately high terrace units.

3.8. Pollution load index (PLI)

PLI was determined for each sample and showed that PLI was >1 in most soil samples, indicating that they are polluted (Fig. 15, Table 8).

3.9. Degree of Contamination (DC)

DC within the study area ranged from 13.83 to 69.07, which indicated that the study area fell into the 'considerable' and 'high' degree of contamination classes (Fig. 15, Table 8).

Where:

L = Low contamination class.

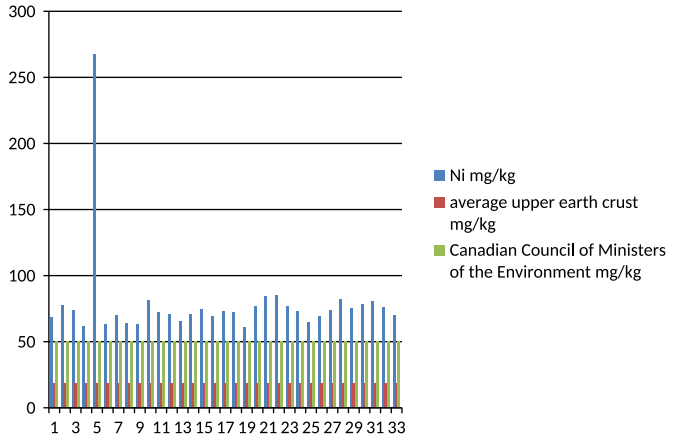

Fig. 10. Nickel concentrations in soil samples and concentration limits specified by Wedepohl (1995) and CSQG (2007).

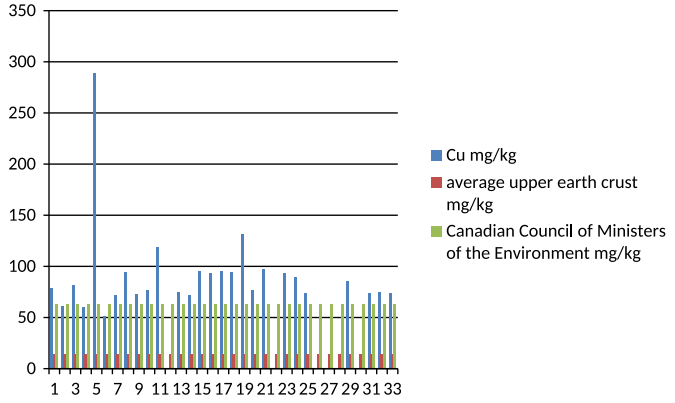

Fig. 11. Copper concentrations in soil samples and concentration limits specified by Wedepohl (1995) and CSQG (2007).

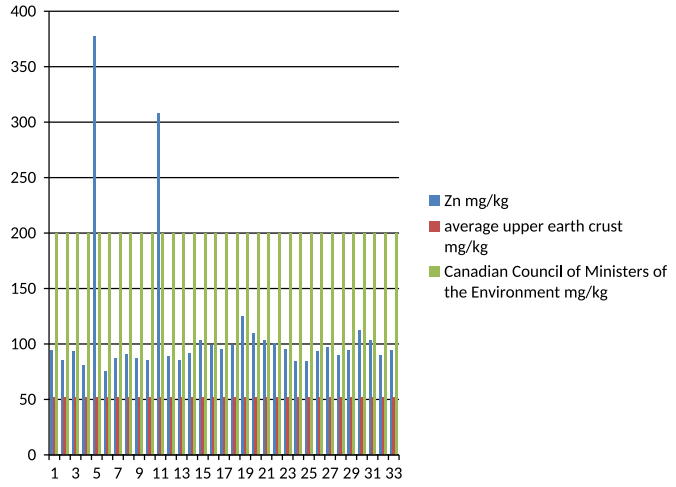

Fig. 13. Zinc concentrations in soil samples and concentration limits specified by Wedepohl (1995) and CSQG (2007).

M = Moderately contaminated class.
C = Considerably contaminated class.
VH = Very highly contaminated class.

4. Conclusions

All heavy metals in the study area exceeded the crustal mean values specified by Wedepohl (1995). Ni and Cr concentrations exceeded recommended values in all soil profile horizons (CSQG, 2007), while Cu had a variable distribution. Zn concentrations are under recommended concentration limits in most soil samples. The CF values of V were in the 'considerably' and 'very highly' contaminated Classes. According to the CF results, the Cr concentrations of all samples are in the 'considerably' and 'very highly' contaminated Classes. The CF for Ni shows that all samples are in the 'considerably' and 'very highly' contaminated classes. For Cu, soil samples were in three contamination classes ('low,' 'considerably' and 'very highly' contaminated). All Zn concentrations in all soil samples fell into the 'moderately contaminated' class, except for the first horizons of Profiles 2 and 4, which were

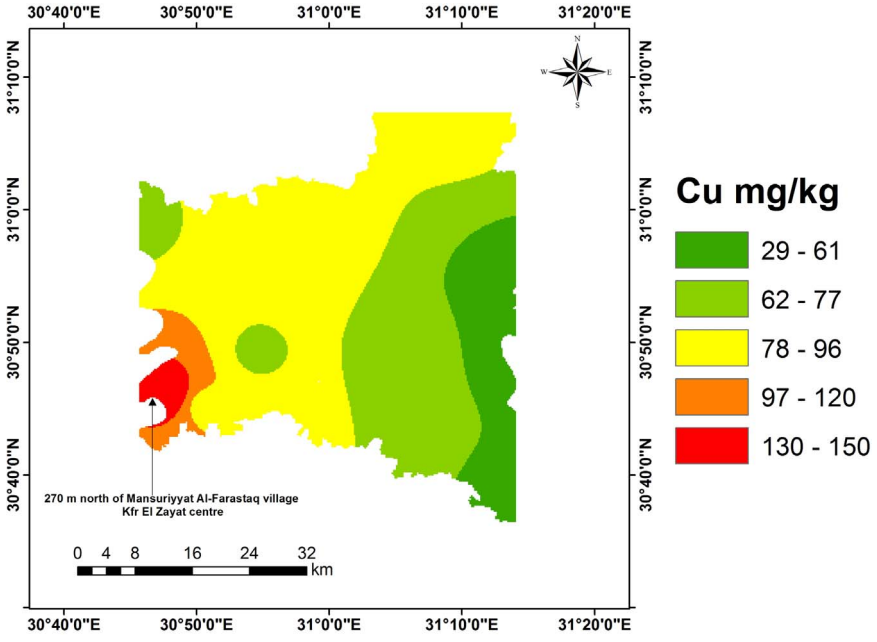

Fig. 12. The interpolated map of weighted mean of copper.

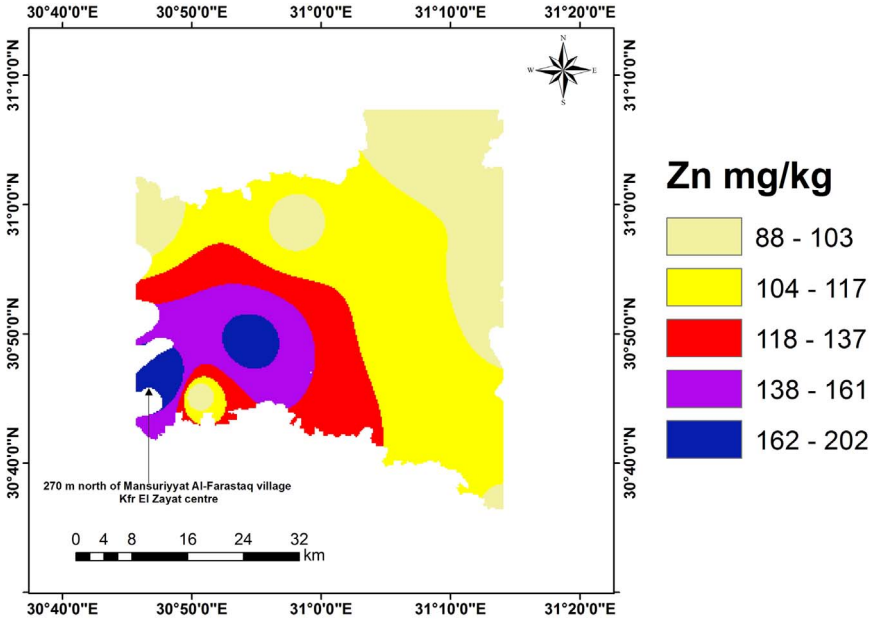

Fig. 14. The interpolated map of weighted mean of zinc.

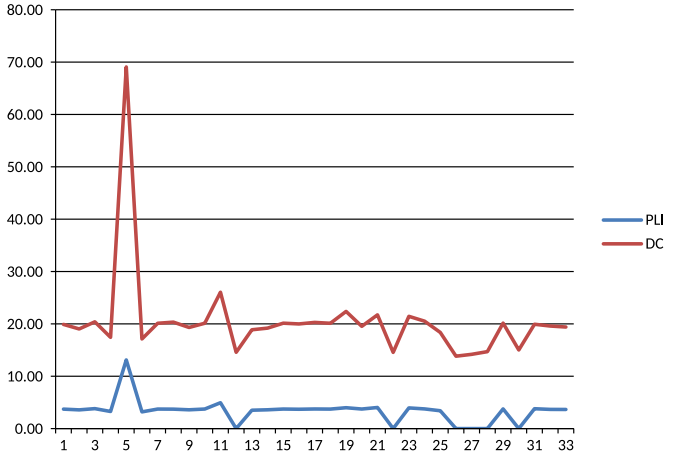

Fig. 15. The Pollution Load Index (PLI) and Degree of Contamination (DC) of study area soils.

in the 'very highly' and 'considerably contaminated' classes, respectively. The Pollution Load Index was >1 in most soil samples, indicating a pollution problem. The study area fell into two classes ('considerable' and 'high' degree of contamination). In terms of the distribution of heavy metals in the different physiographic units, the swale units contained the highest concentrations, probably due to the many factories located in this unit. This research recommends that heavy metal contamination should be investigated within entire soil profiles and not just top-soils, because of the high mobility of these metals, which could affect soil and crop quality and can cause groundwater pollution. In order to prevent soil and water pollution and to avoid the need for costly remediation in the future, precise measures and efficient methods to improve soil and water quality must be implemented.

Acknowledgement

The authors thank The Egyptian Ministry of Higher Education (Cultural Affairs and Missions Sector) for funding the PhD programme of Mr. Mohamed S. Shokr.

Table 8
The Pollution Load Index (PLI) and Degree of Contamination (DC) of study area soils.

Profile no	Depth	PLI	DC
1	0–50	3.72	19.90
	50–85	3.58	19.03
	85–120	3.81	20.39
	120–150	3.27	17.43
2	0–45	13.11	69.07
	45–85	3.19	17.12
	85–110	3.73	20.11
3	0–75	3.71	20.33
	75–100	3.59	19.32
	100–150	3.74	20.12
4	0–60	4.94	26.04
	60–100	0.00	14.57
	100–120	3.51	18.87
	120–150	3.59	19.19
5	0–45	3.74	20.13
	45–65	3.70	19.99
	65–110	3.75	20.28
	110–150	3.72	20.11
6	0–35	3.99	22.38
	35–65	3.74	19.53
	65–100	4.03	21.72
	100–150	0.00	14.55
7	0–55	3.95	21.44
	55–110	3.76	20.52
	110–150	3.41	18.37
8	0–30	0.00	13.83
	30–60	0.00	14.18
	60–100	0.00	14.70
	100–150	3.76	20.15
9	0–45	0.00	15.02
	45–105	3.79	19.93
	105–130	3.67	19.59
	130–150	3.65	19.40

References

Abdelhafez, A. A., Abbas, H. H., Abd-El-Aal, R. S., Kandil, N. F., Li, J., & Mahmoud, W. (2012). Environmental and health impacts of successive mineral fertilization in Egypt. *Clean Soil Air Water*, *40*(4), 356–363.

Abdelhafez, A. A., & Li, J. (2014). Geochemical and statistical evaluation of heavy metal status in the region around Jinix River, China. *Soil and Sediment Contamination*, *23*, 850–868.

Abdel-Moati, M. A. R., & El-Sammak, A. A. (1997). Man-made impact on the geochemistry of the Nile Delta Lakes. A study of metal concentrations in sediments.

Water, Air and Soil Pollution, *97*(3), 413–429.
Abrahams, P. W. (2002). Soils: Their implications to human health. *The Science of the Total Environment*, *29*, 11–32.
Ali, A. A., & Moghanm, F. S. (2013). Variation of soil properties over the landforms around Idku Lake, Egypt. *The Egyptian Journal of Remote Sensing and Space Sciences*, *16*(1), 91–101.
Baghdady, N. H., & Sippola, J. (1984). Extractability of polluting elements Cd, Cr, Ni and Pb of soil with three methods. *Acta Agriculturae Scandinavica*, *34*(3), 345–348.
Ball, D. F. (1964). Loss-on-ignition as estimate of organic matter and organic carbon in non-calcareous soils. *Journal of Soil Science*, *15*(1), 84–92.
Buekers, J. (2007). *Fixation of cadmium, copper, nickel and zinc in soil: kinetics, mechanisms and its effect on metal bioavailability* (Ph.D. thesis) Leuven, Belgium: Catholic University of Leuven.
Caeiro, S., Costa, M. H., & Ramos, T. B. (2005). Assessing heavy metal contamination in Sado Estuary sediment: An index analysis approach. *Ecological Indicators*, *5*, 151–169.
Canadian Soil Quality Guidelines (CSQG)(2007). Canadian Soil Quality Guidelines (CSQG) for the Protection of Environmental and Human Health: Summary tables. Updated September, 2007. In: Canadian Environmental Quality Guidelines, 1999, Canadian Council of Ministers of the Environment (CCME), Winnipeg.
Climatologically Normal for Egypt (2011). The Normal for El-Gharbia Governorate Station (1960–2011), Ministry of Civil Aviation: Meteorological.
D'Amore, J., Al-Abed, S. R., Scheckel, K. G., & Ryan, J. A. (2005). Methods for speciation of metals in soils: a review. *Journal of Environmental Quality*, *34*(5), 1707–1745.
Desaules, A. (2012). Critical evaluation of soil contamination assessment methods for trace metals. *Science of the Total Environment*, *426*, 120–131.
Dobos E., Norman B., Bruce W., Luca M., Chris J., & Erika M.(2002). The use of DEM and satellite images for regional scale soil database. 17th World Congress of Soil Science (WCSS), 14-21 August, Bangkok, Thailand.
El-Bady, M. S. (2014). Spatial distribution of some important heavy metals in the soils south of Manzala Lake in Bahr El-Baqar Region, Egypt. *Nova Journal of Engineering and Applied Sciences*, *3*(2), 1–12.
FAO (2006). Guidelines for Soil Description, 4th edn. FAO, Rome. ISBN 92-5-105521-1.
Hakanson, L. (1980). An ecological risk index for aquatic pollution control. A sedimentological approach. *Water Research*, *14*, 975–1001.
ITT (2009). ITT Corporation ENVI 4.7 Software, White Plains: New York.
Jankaitė, A., Baltrėnas, P., & Kazlauskienė, A. (2008). Heavy metal concentrations in roadside soils of Lithuania's highways. *Geologija*, *50*(4), 237–245.
Kaasalainen, M., & Yli-Halla, M. (2003). Use of sequential extraction to assess metal partitioning in soils. *Environmental Pollution*, *126*(2), 225–233.
Lillesand, T. M., & Kiefer, R. W. (2007). *Remote Sensing and Image Interpretation* (5th ed.) New York: John Wiley.
Mbah, C., & Anikwe, M. (2010). Variation in heavy metal contents on roadside soils along a major expressway in south east Nigeria. *New York Science Journal*, *3*(10), 103–107.
Omran, E. S., & El Razek, A. (2012). Mapping and screening risk assessment of heavy metal concentrations in soils of the Bahr El-Baker Region, Egypt. *Journal of Soil Science and Environmental Management*, *6*(7), 182–195.
Parveen, N., Ghaffar, A., Shirazi, S. A., & Bhalli, M. N. (2012). A GIS based assessment of heavy metal contamination in surface soil of urban parks: A case study of Faisalabad City-Pakistan. *Journal of the Geography of Natural Disasters*, *2*, 5.
Reimann, C., & de Caritat, P. (2000). Intrinsic flaws of element enrichment factors (EFs) in environmental geochemistry. *Environmental Science and Technology*, *34*, 5084–5091.
Said, R. (1993). *The River Nile: Geology, Hydrology and Utilization* Oxford: Pergamon Press.
Senesi, G. S., Baldassarre, G., Senesi, N., & Radina, B. (1999). Trace element inputs into soils by anthropogenic activities and implications for human health. *Chemosphere*, *39*, 343–377.
Seshan, B. R. R., Natesan, U., & Deepthi, K. (2010). Geochemical and statistical approach for evaluation of heavy metal pollution in core sediments in southeast coast of India. *International Journal of Environmental Science and Technology*, *7*(2), 291–306.
Shepard, D. (1968). *A Two-dimensional Interpolation Function for Irregularly-spaced Data* New York: ACM.
Sofianska, E., Michailidis, K., Mladenova, V., & Filippidis, A. (2013). Multivariate statistical and GIS-based approach to identify heavy metal sources in soils of the Drama Plain, Northern Greece. *Geoscience Journal*, 131–132.
Tomlinson, D. C., Wilson, D. J., Harris, C. R., & Jeffrey, D. W. (1980). Problem in assessment of heavy metals in estuaries and the formation of pollution index. *Helgol Wiss Meeresunlters*, *33*(1–4), 566–575.
USDA (2010). Keys to Soil Taxonomy. United States Department of Agriculture, Natural Resources Conservation Service (NRCS), 11th Edition.
Wedepohl, K. H. (1995). The composition of the continental crust. *Geochimica et Cosmochimica Acta*, *59*, 1217–1239. http://dx.doi.org/10.1016/0016-7037(95)00038-2.
Wu, J., Teng, Y., Lu, S., Wang, Y., & Jiao, X. (2014). Evaluation of soil contamination indices in a mining area of Jiangxi, China. *PLoS ONE*, *9*(11), e112917. http://dx.doi.org/10.371/journal.pone.0112917.
Zeydan, B.A. (2005). The Nile Delta in a Global Vision. In: Proceedings of the Ninth International Water Technology Conference, IWTC9 2005, Sharm El-Sheikh, Egypt, 31–40
Zheng, C. (2006). Using multivariate analyses and GIS to identify pollutants and their spatial patterns in urban soils in Galway, Ireland. *Environmental Pollution*, *142*(3), 501–511.